Mineralogy and Petrology (2001) 73: 67–91

Mineralogy and Petrology

Quaternary evolution of the southern sector of the Campanian Plain and early Somma-Vesuvius activity: insights from the Trecase 1 well

D. Brocchini[1], **C. Principe**[2], **D. Castradori**[3], **M. A. Laurenzi**[2], and **L. Gorla**[3]

[1] Piombino (LI), Italy
[2] Istituto di Geoscienze e Georisorse – Area della Ricerca CNR di Pisa S. Cataldo, Pisa, Italy
[3] AGIP S.p.A, San Donato Milanese, Italy

With 5 Figures

Received April 12, 2000;
revised version accepted March 1, 2001

Summary

The present review of data on the Trecase 1 well, including stratigraphy, updated $^{40}Ar/^{39}Ar$ ages and the results of newly performed calcareous nannofossil studies, serves to resolve the chronological contradictions pointed out by Bernasconi et al. (1981) and Balducci et al. (1983) concerning the onset of volcanic activity in the area now occupied by the Somma-Vesuvius Volcanic Complex. New $^{40}Ar/^{39}Ar$ data indicate that volcanic activity in this area started about 0.4 myr B.P. After such time, tephritic magmatic activity, distributed in small scattered centers, developed and alternated with periods of volcanic quiescence and marine sedimentation. This first phase of magmatic activity ended in the Vesuvian area about 0.3 myr B.P. and was followed by a period of marine sedimentation in a marginal environment. Complete emergence of the shoreline occurred about 37,000 yr B.P. as a result of sea level changes during the last glacial period and deposition of the 60 m thick Campanian ignimbrite (CI). Volcanic activity reappeared in the Vesuvian area only after the CI eruption. Magma rising along and at the intersection of linear and curved tectonic and volcano-tectonic elements (linked to the pre-existing Pleistocene tectonic trend and formation of the vast Phlegraean Fields caldera) formed a number of small lava and scoria edifices. One of these tephritic centers lies above the CI deposits under the Trecase 1 well area. The CI bottom in the Trecase 1 well is currently at an altitude of −120 m a.s.l.; this allows estimating the maximum tectonic subsidence over the last 37,000 yr. by the southern sector of the Vesuvian area to be about 30 m.

Introduction

The well "Trecase 1" (Fig. 1) was drilled on the southern slope of Mt. Vesuvius (40° 47′ 07″ N; 14° 26′ 40″ E) by AGIP SpA between November 1980 and March 1981, to explore the volcano's geothermal resources under the terms and provisions of a joint venture between AGIP and ENEL. The rotary table was set at 220 m a.s.l. The well, which was drilled to a maximum depth of 2072 meters, was not only dry, but also cold. It was therefore shut down and abandoned.
However, the drill hole represents an important source of geological information, particularly because:

i) it is the only well drilled in the Campanian Plain which has encountered the Mesozoic basement carbonate rocks;
ii) the physical characteristics of the rock sequence drilled in the well constitute the ground reference for calibration of all geophysical models of the Campanian Plain;
iii) the succession of deposits encountered by the well provides important information on the various phases of volcanic activity that has consistently contributed to the filling of this sector of the Campanian Plain;
iv) its location outside the area affected by caldera collapse and its considerable depth make it the only current source of undisturbed stratigraphic information on the origins and evolution of volcanic activity in the Somma-Vesuvius volcanic complex (hereafter, the Vesuvian area).

However, despite its obvious importance, only two papers concerning the Trecase 1 well have been published over the last 20 years or so. The first is a short preliminary description of its stratigraphy and geochronology (*Bernasconi* et al., 1981), while the second is a review of data related to the drilling history (*Balducci* et al., 1983).

All subsequent geological literature on the Campanian Plain refers to the preliminary and somewhat controversial information contained in these two papers. Since the Trecase 1 well was drilled, important progress has been made in our understanding of the geological evolution of the Campanian Plain, and of the volcanic history of Somma-Vesuvius.

The aim of this paper is to review the stratigraphy of the Trecase 1 well as well as new isotopic age determinations and calcareous nannofossil studies.

Geological outline

The geological evolution of the Campanian Plain (Fig. 1) and its correlation with volcanic activity in this part of Italy have been the subject of numerous publications (*Ippolito* et al., 1973; *Ortolani* and *Aprile*, 1978; *Cinque* et al., 1987, 1993; *Albore Livadie* et al., 1989; *Barra* et al., 1989; *Brancaccio* et al., 1991; *Cinque*, 1991; *Romano*, 1992). More recently, detailed studies have also been conducted on the stratigraphy of the many water wells drilled in the Campanian Plain, particularly in its southern sector (*Bellucci*, 1994 and 1998; *Di Vito* et al., 1998a,b).

The total absence of Pliocene marine sediments in the drilled sequence of the Trecase 1 well, and outcrops of a Late Pliocene/Early Pleistocene erosional surface

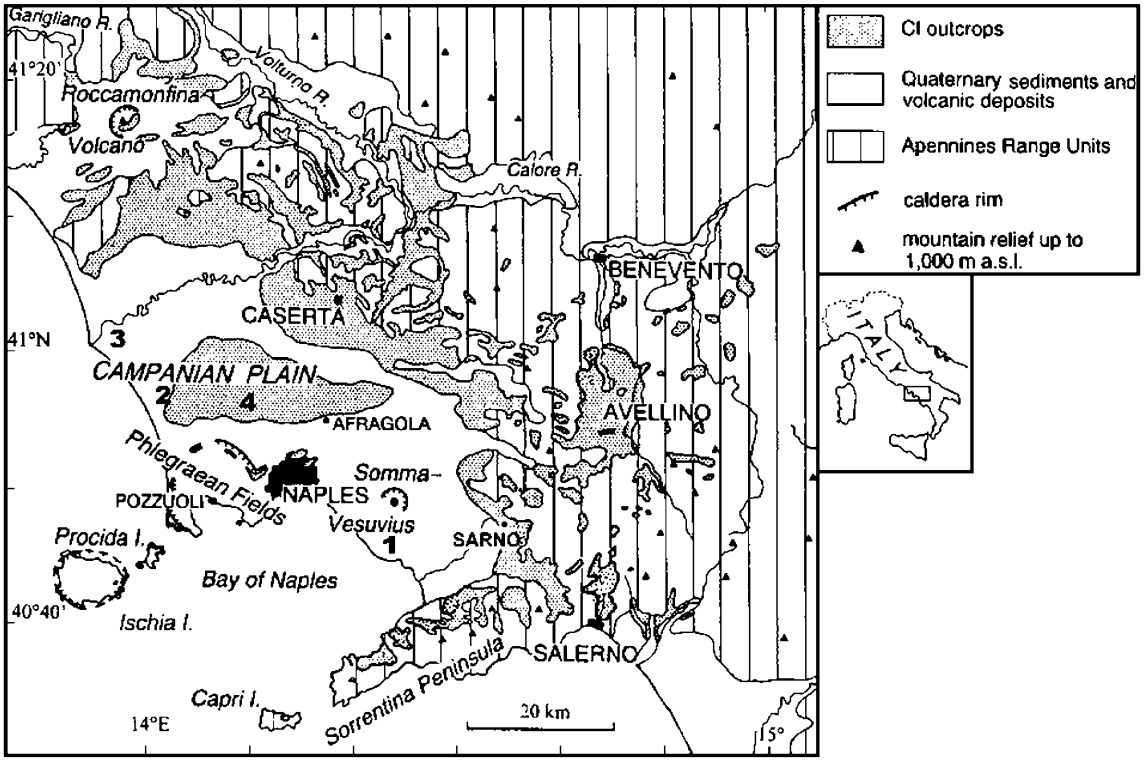

Fig. 1. The Southern sector of the Campanian Plain. *1* Trecase 1 well; *2* Villa Literno 1 well; *3* Castel Volturno 1 well; *4* Parete 2 well (modified from *Rosi* et al., 1999)

indicate that the southern part of the Campanian Plain and the River Sele were above sea level during the Pliocene (*Brancaccio* et al., 1991; *Cinque* et al., 1993).

Starting from the lower part of the Early Pleistocene, the Campania-Lucania segment of the Southern Apennines was affected by tectonism which now facilitates subdivision into an outer, an axial and an inner zone (*Cinque* et al., 1993). While the outer and axial zones reveal tilting of the pre-Pleistocene sedimentary formations, the latter in the inner zone are affected by subsidence. Strike-slip fault tectonics and associated tension gashes have contributed to these developments.

Since the Middle Pleistocene NE-SW extension has prevailed over the strike-slip fault tectonics in the Campanian Plain area (*Brancaccio* et al., 1991; *Hippolyte* et al., 1994).

Geophysics also shows displacements of the chain units (here represented mainly by Mesozoic carbonate rocks) (*Finetti* and *Morelli*, 1974; *Cassano* and *La Torre*, 1987 and references therein; *Berrino* et al., 1998; *Bruno* et al., 1998). A number of deep wells has been drilled in the middle of the Campanian Plain (Fig. 1) to a maximum depth of 3000 m (Castel Volturno 1) without encountering the carbonate basement (*Ippolito* et al., 1973; *Ortolani* and *Aprile*, 1978), which becomes deeper towards the center of the Plain. The Parete 2 and Villa Literno 1 deep wells, have revealed the presence of a huge volcanic massif with calc-alkaline affinity and a K/Ar age of 2 ± 0.4 myr (*Di Girolamo* et al., 1976; *Barbieri* et al., 1979).

The Sorrentina peninsula, which is the south-eastern limit of the Campanian Plain (Fig. 1), has been subjected to similar tectonic evolution as the inner zone since the Lower Pleistocene. However, it presents right-lateral strike-slip faults with no associated tensional component.

Subsidence in the Campanian Plain continued during the Upper Pleistocene and Holocene (*Brancaccio* et al., 1991). During this period volcanic activity began in different volcanic centers in both the Campanian Plain and adjacent areas, such as Ischia (*Gillot* et al., 1982) and the Phlegraean Fields (*Rosi* and *Sbrana*, 1987). Tephra deposits interbedded with marine sediments, thus furnishing important stratigraphic and geo-chronological markers.

About 37,000 yr B.P. (*Deino* et al., 1992, 1994), an extremely violent explosive eruption produced the Campanian ignimbrite (CI) and the concomitant collapse of the Phlegraean Fields caldera (*Rosi* et al., 1983).

The CI uniformly covered the entire Campanian Plain with a thickness of several tens of meters, while an even thicker cover is found in the proximal area (caldera rim facing Naples). Deposition also occurred against the bordering limestone terrain (*Orsi* and *Rosi*, 1991). As a consequence of the voluminous CI deposition the entire Campanian Plain aggraded (*Di Vito* et al., 1998a). Numerous scoria cones and leucite lavas on top of the CI are the result of effusive activity. Thus, the Campanian Plain was subdivided into a series of different sedimentation domains (*Di Vito* et al., 1998a). Overlying those effusive centers are some fallout deposits attributed to the Vesuvian eruption of Pomici di Base (*Di Vito* et al., 1998b). Radiocarbon ages, of the underlying paleosol, give 18,000 yr B.P. to 19,000 yr B.P. (Table 1; *Andronico* et al., 1995; *Bertagnini* et al., 1998). A plinian fallout deposit within the tephra sequence following the CI eruption in the Plain is an important stratigraphic marker, related to the Phlegraean Fields eruptions of Pomici Principali (*Di Vito* et al., 1998b), whose age is of the order of 10,000 yr B.P.

Table 1. *Radiocarbon and* $^{40}Ar/^{39}Ar$ *ages of the main eruptions of Phlegraean Fields (CF) and Somma-Vesuvius (SV). Data from* Andronico *et al., 1995 (a);* Delibrias *et al., 1979 (b);* Rosi *et al., 1987 (c);* Cassignol *and* Gillot, *1982 (d);* Bertagnini *et al., 1998 (e);* Deino *et al., 1992 and 1994 (f)*, Gans *et al., 1999 (g)*

Eruption	Volcano	Method	Age (yr BP)	Reference
Pompei (79 AD)	SV	^{14}C	2,030±30	(a)
Avellino	SV	^{14}C	3,360±40	(a)
Mercato (*)	SV	^{14}C	8,010±35	(a)
Pomici Principali	CF	^{14}C	9,500–11000	(b)
Neapolitan Yellow Tuff	CF	^{14}C	11,200–11,300	(c)
		K/Ar	13,800–15,400	(d)
Pomici Verdoline	SV	^{14}C	16,780±170	(a)
Pomici di Base	SV	^{14}C	18,300±180	(a)
		^{14}C	18,750±420	(e)
		^{14}C	19,170±420	(e)
Campanian Ignimbrite	CF	$^{40}Ar/^{39}Ar$	37,100±400	(f)
		$^{40}Ar/^{39}Ar$	39,180±120	(g)

(*) Ottaviano eruption in *Rolandi* et al. (1993a)

(Table 1; *Rosi* and *Sbrana*, 1987). Above, there are: i) marine and transition sediments of the Versilian transgression, during which the sea entered the Sarno Plain as far as Scafati, 2 km east of Pompeii (*Cinque*, 1991); ii) pyroclastic deposits from the activity of the Phlegraean Fields and some major eruptions of Vesuvius (*Di Vito* et al., 1998a); iii) swamp deposits and travertine layers (*Di Vito* et al., 1998a).

The Somma-Vesuvius volcanic activity of about 10,000 yr ago is represented by numerous explosive events of varying magnitude, among which the Mercato, Avellino and Pompeii episodes (Table 1) stand out in terms of volumes deposited. The most recent deposits cropping out in the area of the Trecase 1 well are those related to Vesuvius' historically documented effusive activity (*Principe* et al., 1987).

Stratigraphy

Although the Trecase 1 well reached a maximum depth of 2072 meters (from the rotary table), the deepest recovered cuttings are from a depth of 2068 meters (Fig. 2). In order to improve the reliability of the stratigraphic correlations with the volcanic outcrops in the Vesuvian area, study of the stratigraphic sequence encountered by the Trecase 1 well has been conducted through both the analysis of thin sections (cuttings and core samples), as well as reflected light observation of the cuttings.

Stratigraphy from 0 to 532 m

This interval is characterized by the predominance of volcanic material (Fig. 2).

Little information is available in the final drilling report on the uppermost 200 m (*Agip*, 1981). Frequent and considerable loss of circulation was experienced here, preventing recovery of the majority of the cuttings. The consistent loss of circulation suggests the presence of loose, highly permeable tephra beds and/or fractured and scoriaceous lava flows in this shallow section of the well.

Only few levels were described in this interval:

- 44–56 m: predominance of tuff
- 56–60 m: leucite porphyritic lava
- 60–74 m: ''chaotic tuff''
- 74–86 m: hypocrystalline basic lava with some bubbles and argillified and oxidized groundmass
- 106–116 m: argillified cineritic tuff with leucite and plagioclase phenocrysts
- 140–150 m: hypocrystalline lava flow rich in mafic minerals and with a partially argillified groundmass
- 174–194 m: possible intercalations of lava and tephra. At least one hypocrystalline lava flow with leucite and mafic minerals has been encountered

From 200 to 250 m: There are four lava flows within this 50-meter interval of the sequence, each of which is separated by scoriaceous levels and thin intercalations of tephra containing fragments of a microcrystalline glassy matrix, white sanidine porphyritic pumice and sanidine crystals. The lava flows differ one from the other in the amount of vesiculs and the amount and size of the mineral phases present. There

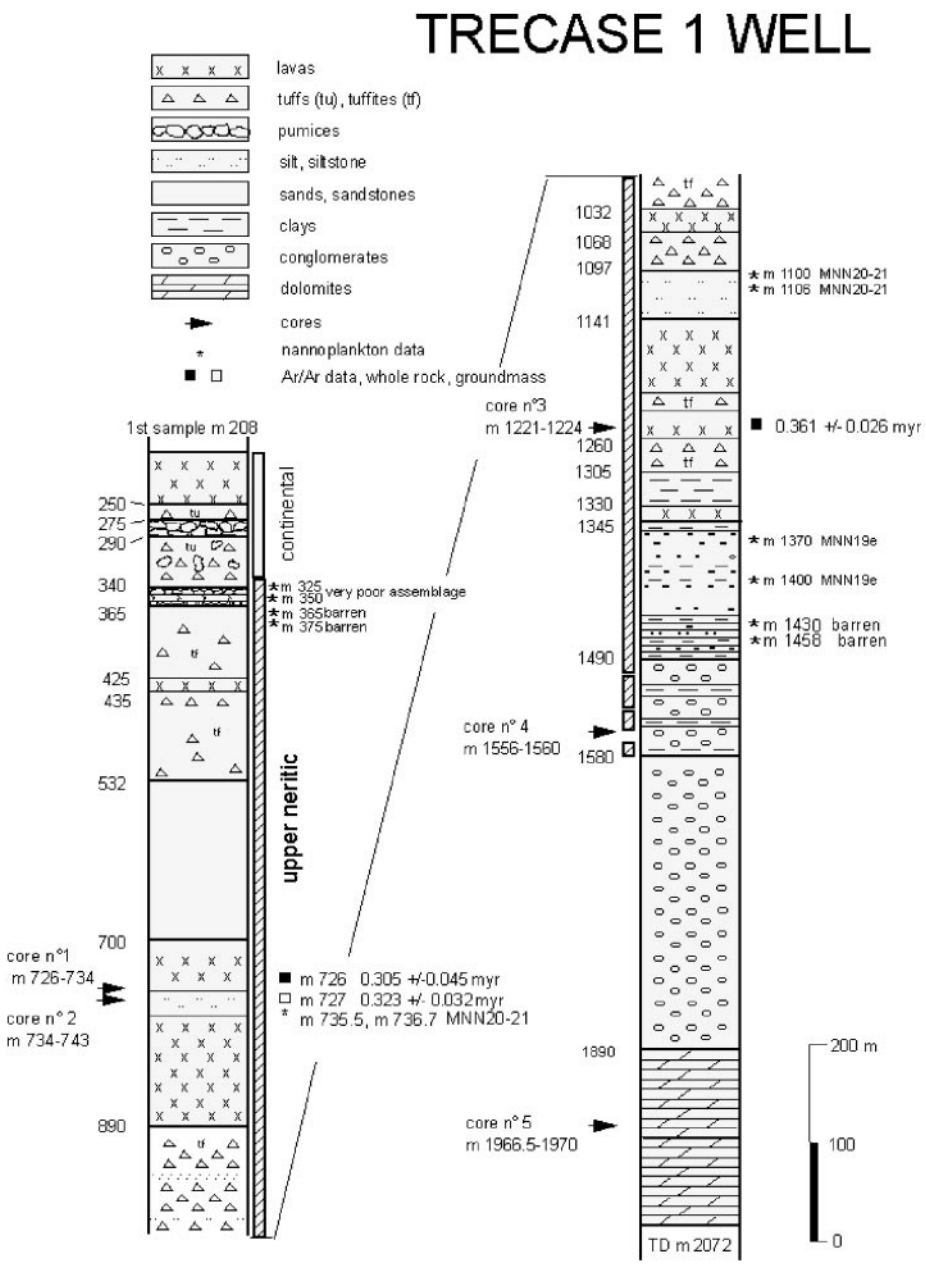

Fig. 2. Trecase 1 well stratigraphy based on cuttings and cored samples

is clinopyroxene and leucite phenocrysts and minor olivine. The uppermost lava flow is characterized by the presence of numerous millimeter-sized clinopyroxene and olivine phenocrysts. Leucite is also present as microphenocrysts, while abundant plagioclase microlites are also present in the two lowermost lava flows.

From 250 to 290 m: From 250 to 275 m there is a light gray pumice tuff with a homogeneous, fine-grained matrix and loose idiomorphic, bright green-colored pyroxene crystals, olivine, sanidine and stretched white pumice particles. Then,

from 275 to 290 m, light stretched pumice, sanidine and porphyritic clinopyroxene predominate and represent a well-defined fallout layer. Numerous fragments of dark glass with feldspar and pyroxene microlites are also present. At 290 m vesiculated dark glass and porphyritic sanidine are still present.

From 290 to 340 m: Yellowish tuff containing slightly stretched pumice, porphyritic sanidine and clinopyroxene. Millimeter-sized sanidine crystals are scattered throughout the groundmass together with fragments of vesiculated dark glass (sometime with stretched bubbles). Lithic clasts, including lavas, are abundant. At 320 m the tuff becomes finer, gray-colored and the amount of dark mica increases. At 335 m, light and dark limestones are present among the lithic clasts.

The tuff matrix is somewhat clayey, while the pumice glass appears unaltered, light and clear.

From 340 to 345 m: Sanidine, clinopyroxene, biotite and olivine porphyritic white pumice; millimeter-sized, loose crystals of sanidine with glassy inclusions, clinopyroxene and olivine, obsidian glass with sanidine and limestone. The pumice glass appears to be clayey.

From 345 to 365 m: At 345 m, coarse-grained holocrystalline lava. From 355 to 365 m a fine tuff with abundant fractured sanidine crystals is present, together with fragments of perlitic and obsidian glass, dark mica and elongated bright green crystals of clinopyroxene.

From 365 to 532 m: Down to 365 m there is a succession of sands with decreasing amounts of volcanic components (loose crystals of sanidine and clinopyroxene, well-stretched white pumice, dark glass, obsidian and fine-grained tuffites). The sands also contain sporadic fragments of shells of the genus Cardium. Between 425 and 435 m there is a light gray-colored microcrystalline lava which represents the only volcanic product of primary emplacement within this interval. Starting at 460 m depth numerous oolites appear; initially their cores are made up of sanidine crystals and subsequently of calcareous fragments.

Stratigraphy from 532 to 2068 m

From 532 to 700 m: Alternating sands with different grain sizes made up of macro- and micro-fossil fragments, micritic limestone, quartz sandstone and sanidine crystals. At 620 m there is a level of light, aphyric, vesiculated glass fragments. Lava fragments first appear at 690 m and are mainly tephritic and, to a lesser degree, latitic.

From 700 to 890 m: Predominance of tephritic lava flows with modal leucite. The lava flows are intercalated with some siltstones and tuffites (volcanogenic sediments). The main siltstone layer is from 734 to 743 m. Lavas are mostly fine-grained with phenocrysts of plagioclase, clinopyroxene and olivine, while the groundmass consists of clinopyroxene, leucite, plagioclase, magnetite, rare biotite and sanidine. The presence of some scoriaceous layers, especially in the lower part of this interval, suggest pile-up of cooling lava flow units.

From 890 to 1097 m: Predominance of tuffites with interbedded tephritic lavas (from 1032 to 1068 m). The tuffites are mixed with fine-grained, carbonate-matrix sandstones and siltstones with variable clay contents.

From 1097 to 1141 m: Carbonate-cemented, clayey siltstone containing tufitic material, aphiric dark glass and rare fossils.

From 1141 to 1345 m: The clays from 1307 to 1330 m represent deep-sea episode in this sequence. The beginning of effusive volcanic activity in the submerged Campanian Plain is marked by lava flows from 1330 to 1345 m. These lava flows are petrographically very similar to those found in the 700–890 m interval.

From 1345 to 1490 m: Alternating siltstones and calcarenites with numerous macro- and micro-fossils, indicating a marine environment. From 1388 to 1391 m there is a layer of glassy fragments, almost fully replaced by calcite, which contains sanidine phenocrysts.

From 1490 to 1580 m: Limestone conglomerate with fragments of dolostone, oolitic and micritic limestone, but no matrix.

From 1580 to 1882 m: A second carbonate-matrix conglomerate unit is present. Clasts consist of fragments of limestone/dolostone.

From 1882 to 2068 m: Micro- and macro-crystalline, gray slightly clayey azoic dolostones. Sulfide impregnations are present.

Ar/Ar Geochronology

Previous chronological data

Previous age determinations on Trecase 1 well samples (Table 2) were obtained through the study of calcareous nannofossil associations from the siltstone layers at 775, 1400 and 1450 m and from the K/Ar radiometric dating of lava collected at 1221 m (*Bernasconi* et al., 1981). The fossils indicate a minimum age of 0.5 myr for the siltstone at 775 m and an age between 0.9 and 1.1 myr for the much deeper siltstones (1400 and 1450 m). The K/Ar age of the 1221 m lava was measured on two separate pieces of the same sample, which yielded 0.27 ± 0.03 myr and 0.3 ± 0.05 myr B.P. The evident discrepancy between K/Ar and nannoplankton dating and the reversed vertical component of the Earth's magnetic field in the cores from 755 m and 1221 m (*Bernasconi* et al., 1981) have cast doubt over the validity

Table 2. *Ages from* Bernasconi *et al. (1981) on Trecase 1 well samples*

Sample	Depth (m)	Method	Results
Lava	755	Paleomagnetism	Reversed vertical magnetic component
Siltstone	775	Calcareous nannofossils biostratigraphy	>0.5 myr
Lava	1221	K/Ar age	0.27 ± 0.03 myr
	1221	K/Ar age	0.3 ± 0.05 myr
Lava	1221	Paleomagnetism	Reversed vertical magnetic component
Siltstone	1400	Calcareous nannofossils biostratigraphy	0.9–1.1 myr
Siltstone	1450	Calcareous nannofossils biostratigraphy	0.9–1.1 myr

of the K/Ar ages. Therefore, in order to establish whether or not such K/Ar data can, in fact, be considered valid, new radiometric age measurements have been performed with the $^{40}Ar/^{39}Ar$ method; thus, it is possible to determine whether the system has been closed since crystallization of the rock.

Petrochemistry of the analyzed samples

Various alteration processes can affect the original potassium content of the mineral phases present in a rock, thus producing variations in the isotope ratios utilized for age determinations with the $^{40}Ar/^{39}Ar$ method. In order to verify the degree of alteration (whole-rock and single mineral phases), the following analyses have been carried out: i) petrographic study; ii) whole-rock XRF analyses (Table 3); iii) microprobe analyses of the mineral phases present (Table 4).

The resulting LOI values are high for the 726 m and 727 m samples (4.07 and 5.68%, respectively) and lower for the 1221 m lava (1.44%). The lava at 726 m depth has an aphyric texture with rare plagioclase, clinopyroxene and olivine phenocrysts, the latter being almost completely altered. Plagioclase, leucite, clinopyroxene, sanidine, oxides and hydroxides constitute the groundmass. The lava at 727 m depth has a porphyritic texture with leucite, clinopyroxene, plagioclase and olivine; the latter is almost completely replaced by calcite and magnetite. Plagioclase, leucite, clinopyroxene, magnetite, hydroxides and dark glass constitute the groundmass. The lava at 1221 m depth consists of rare plagioclase and clinopyroxene glomero-porphyric assemblages, and some altered olivine. Clinopyroxene, leucite, plagioclase, biotite, sanidine, oxides and hydroxides constitute the groundmass. Clinopyroxene carries apatite inclusions.

Phenocrysts in the lavas from 726 and 1221 m depth are not altered except for olivine; secondary calcite is present in the groundmass. At 727 m calcite in the groundmass is more abundant and the leucite phenocrysts are altered. Secondary minerals (calcite, oxides and hydroxides) present in all three lavas probably result in

Table 3. *Major-element XRF analyses of the* $^{40}Ar/^{39}Ar$ *dated Trecase 1 lavas. Analyses were performed at the Department of Earth Sciences, University of Pisa*

Sample	726 m	727 m	1221 m
SiO_2	50,20	48,70	46,44
TiO_2	1,01	1,03	1,10
Al_2O_3	17,19	16,97	18,24
Fe_2O_3	4,58	3,48	3,18
FeO	3,33	3,92	5,07
MnO	0,14	0,13	0,17
MgO	3,05	3,62	4,30
CaO	7,10	8,22	9,72
Na_2O	2,25	3,77	2,61
K_2O	6,03	3,44	6,14
P_2O_5	0,61	0,56	1,05
LOI	4,07	5,68	1,44
Total	99,56	99,53	99,47

Table 4. *Microprobe analyses of plagioclase, leucite, pyroxene, biotite and sanidine of the lavas dated. (n) = number of analyses. Oxides represent the average value of the analytical data. Analyses were performed on a Cameca-Camebax electron microprobe at the CSGA-CNR in Padua. Acceleration voltage was 15 kV, beam current 15 nA, beam diameter* 1 μm

	Plagioclase				Leucite		Pyroxene				Biotite	Sanidine
	$726_{(12)}$	$727_{(5)}$	$727_{(13)}$	$1221_{(6)}$	$727_{(2)}$	$1221_{(13)s}$	$726_{(4)}$	$727_{(4)}$	$1221_{(15)}$	$727_{(13)}$	$1221_{(6)}$	$1221_{(3)}$
SiO_2	45,85	49,57	48,52	46,09	59,65	55,70	49,65	50,27	48,15	48,99	35,40	64,22
TiO_2	0,03	0,09	0,05	0,01	0,10	0,10	1,04	1,01	1,17	1,21	4,71	0,00
Al_2O_3	34,00	31,25	32,14	34,24	24,49	23,88	4,13	4,46	6,55	5,47	13,33	19,91
Cr_2O_3	0,02	0,00	0,01	0,00	0,01	0,01	0,01	0,01	0,03	0,05	0,02	0,00
FeO*	0,58	0,73	0,66	0,61	0,26	0,31	8,08	8,19	6,22	8,11	15,92	0,00
MnO	0,02	0,00	0,02	0,00	0,04	0,02	0,24	0,33	0,12	0,20	0,17	0,00
MgO	0,07	0,06	0,07	0,04	0,02	0,01	13,79	13,91	13,60	13,47	13,17	0,00
CaO	18,57	15,50	16,25	18,62	0,30	0,01	23,02	22,51	24,02	22,64	0,03	0,61
Na_2O	1,02	2,08	2,00	1,08	4,19	0,11	0,20	0,29	0,18	0,30	0,64	2,18
K_2O	0,26	0,81	0,66	0,20	0,28	19,92	0,00	0,00	0,00	0,00	8,09	13,73
Tot	100,42	100,09	100,37	100,88	89,32	100,06	100,15	100,97	100,04	100,45	91,48	100,65

Table 5. $^{40}Ar/^{39}Ar$ *ages of the Trecase 1 lavas*. WR *whole rock;* GM *groundmass. The monitor used was Fish Canyon Tuff biotite, whose age is 27.55 myr (*Lanphere *et al., 1990). Recalculated ages were obtained using the age value proposed by* Cebula *et al. (1986) for the Fish Canyon Tuff (27.84 myr)*

Sample (m)	Age (myr)	Recalculated age (myr)
726 (WR)	0.305±0.045	0.308±0.046
727 (GM)	0.323±0.032	0.326±0.033
1221 (WR)	0.361±0.026	0.369±0.028

part from normal syndepositional alteration processes and in part from cold water interactions. The temperature measured at the well bottom was 59 °C (*Agip*, 1981).

To test the lack of alteration of the mineral phases and, consequently, the distribution of potassium in these samples, microprobe analyses were performed on the plagioclase and clinopyroxene in the three lavas, as well as on the leucite in the 727 m and 1221 m samples and the biotite in the 1221 m sample (Table 4). The leucite of the tephrite lava from 727 m depth has been transformed to analcite, while both the leucite and biotite of the sample from 1221 m depth are unaltered.

Data discussion

The error ($\pm 1\,\sigma$) is due to the low percentage of $^{40}Ar_{rad}$, which for the plateau steps varies between 2.7% and 8.8% (analytical data in Appendix 1). The difference between the plateau age and that calculated on all steps (total age) is an indication of the possible presence of parentless ^{40}Ar. The two values obtained for the lava at 726 m depth diverge quite widely, while for that at 1221 m the two ages coincide within the margin of error ($2\,\sigma$). The release of ^{39}Ar and ^{37}Ar isotopes at different

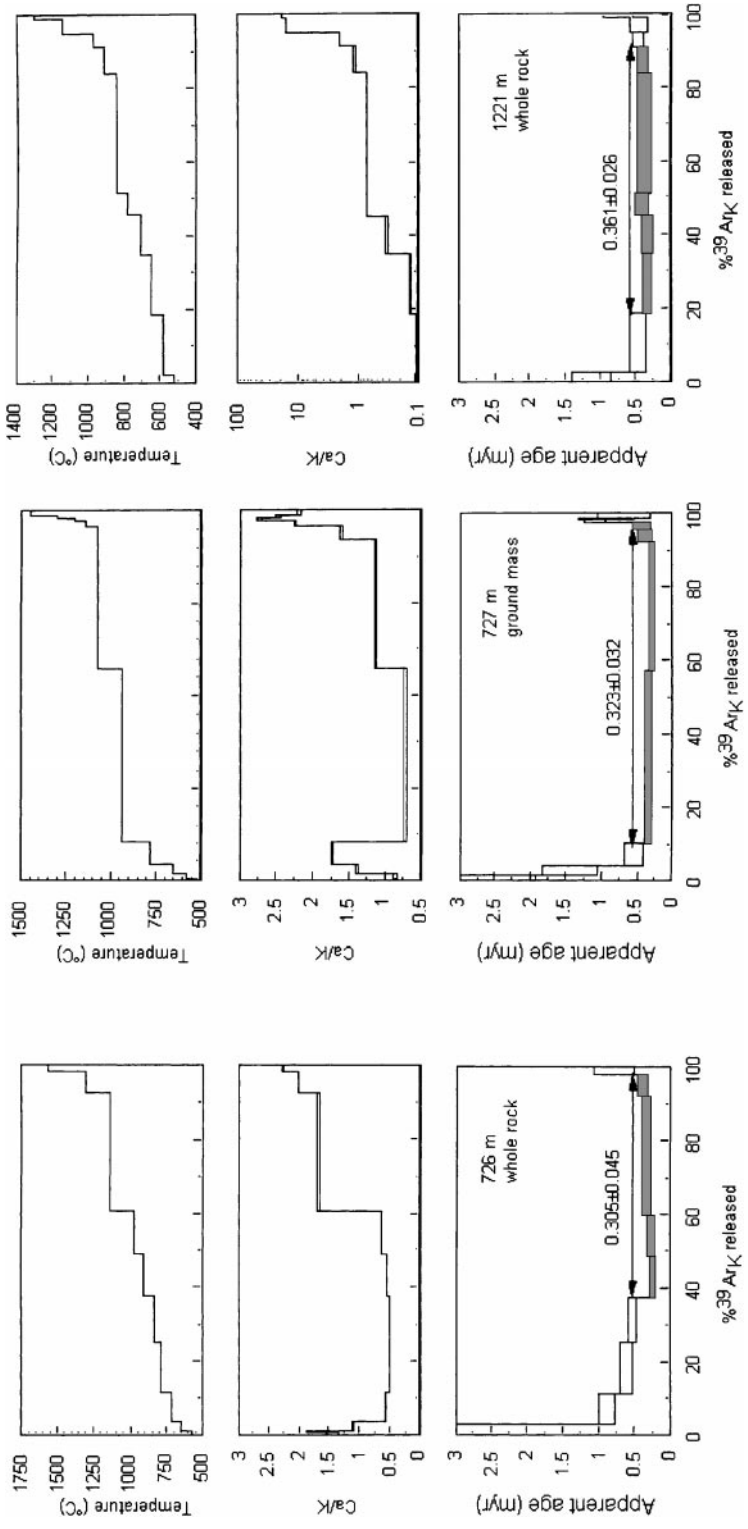

Fig. 3. Apparent age, Ca/K and temperature spectra for the samples analyzed. The plateau date is shown between arrows, which indicate the gas fractions included in plateau calculations. Ca/K is calculated from the ratios of $^{37}Ar_{Ca}/^{39}Ar_K$

heating temperatures is related to mineral chemistry. By comparing the trend of the Ca/K ratio with the electron microprobe data, the kind and degree of phase alterations involved in degassing processes can be assessed. This test is useful in dating rock samples characterized by high LOI values.

Although it is possible to define a plateau for the sample at 726 m depth in the temperature range between 910 and 1300 °C, the spectrum's irregularity, the value of the Mean Standard Weighted Deviation (MSWD = 1.7), and the differences between the plateau ages and the total ages lead to interpreting this spectrum as a saddle. Therefore, the value of 0.305 myr B.P. must be considered the maximum age for this sample. The trend of the Ca/K ratio in the 910–1300 °C steps (Fig. 3) indicates the contemporaneous degassing of sanidine and plagioclase from the groundmass. The increase in this ratio in the high temperature steps indicate the participation of plagioclase and clinopyroxene phenocrysts in the degassing process.

For the sample at 727 m, a plateau is defined at age 0.323 ± 0.032 myr B.P. in the temperature range of 940–1140 °C. Degassing of ^{39}Ar is practically absent at the temperatures at which leucite typically undergoes degassing (< 800 °C), in accord with the alterations revealed by microprobe data for this mineral. The release of ^{39}Ar in this sample is instead concentrated in a plateau interval with Ca/K ratios compatible with the degassing of groundmass plagioclase and glass.

The plateau for the lava at 1221 m depth, with an age of 0.361 ± 0.026 myr B.P., has been defined at between 580 and 910 °C. ^{39}Ar release starts at the degassing temperature typical of leucite (600–800 °C). The Ca/K ratios are very low in this temperature range. Between 800 and 1000 °C the Ca/K ratios are compatible with the contemporaneous degassing of groundmass plagioclase, sanidine and biotite. The considerable increase in the Ca/K ratios at higher temperatures results from the degassing of plagioclase and clinopyroxene phenocrysts.

Comparison of the new value for the $^{40}Ar/^{39}Ar$ total age, 0.408 ± 0.038 myr B.P., with the previously determined K/Ar mean age of 0.285 ± 0.040 shows agreement at the 2σ level.

Calcareous nannofossil biostratigraphy

Recent developments

Shackleton et al. (1990) and *Hilgen* (1991a,b) have defined independent Plio-Pleistocene time scales. They base their chronologies on calibration of different geological proxies (isotopic curves; lithological patterns, such as sapropel-non sapropel or limestone-marl couplets) to the cyclic variation of the Earth's orbital parameters (the so-called ''Milankovitch cycles''; *Imbrie* et al., 1984). Astronomical calibration allows for direct dating, with a precision of about 5,000 yr, of all magnetic reversals from the Brunhes/Matuyama boundary down to the base of the Thvera event (in the lower part of the Gilbert). *Hilgen's* (1991a,b) time scale was then adjusted slightly by *Lourens* et al. (1996) to account for the effect of obliquity on the mainly precession-controlled lithological cycles.

First comparisons between the Astronomic Calibrated Polarity Time Scale (ACPTS) and the Radiometric Calibrated Astronomic Time Scale (RCPTS) (*Hilgen*, 1991a and references therein) demonstrated that the classical K/Ar method

yields age values consistently too low by 5–7%, an unacceptable bias for Pliocene-Pleistocene chronologies.

The discrepancies observed between ACPTS and RCPTS were later explained by using an upgraded age dataset and different statistical approaches (*Tauxe* et al., 1992; *Hall* and *Farrel*, 1995).

Therefore, it is now possible and conceptually correct to compare $^{40}Ar/^{39}Ar$ radiometric datings with biochronological age estimates when the latter are based on the calibration of biohorizons to modern astronomical time scales (*Raffi* et al., 1993; *Castradori*, 1993; *Sprovieri*, 1992, 1993; *Berggren* et al., 1995b).

Trecase 1 well data

Calcareous nannofossil assemblages from 12 samples of the Trecase 1 well have been studied in order to: i) establish the top of marine sediments; ii) obtain age constraints to cross-check the $^{40}Ar/^{39}Ar$ datings.

The samples studied have been subdivided into four groups, and results are discussed accordingly (Fig. 2).

Interval from 325 to 375 m. Four samples (cuttings at 325, 350, 365, and 375 m) were studied in order to establish the top of marine sediments in the well. All samples are characterized by very poor nannofossil assemblages. However, the presence of some specimens of small Gephyrocapsa, a doubtful specimen of Emiliania huxleyi and one of Coccolithus pelagicus in the samples from 325 m depth, suggests that deposition occurred in a (marginal) marine environment. The same applies to the sample from 350 m, characterized by a few small Gephyrocapsa, and normal-sized Gephyrocapsa and Coccolithus pelagicus. The 365 and 375 m samples are practically barren.

Core 2 (734–743 m). Two samples were studied (735.5 and 736.7 m), and the results compared with those reported by *Bernasconi* et al. (1981). The calcareous nannofossil assemblages of the two samples are poor. The almost complete absence of Pseudoemiliania lacunosa (only one, poorly preserved specimen has been observed) suggests correlating this interval with the MNN20–MNN21 Zones of the Middle-Upper Pleistocene (*Rio* et al., 1990). The presence of some small Gephyrocapsa and a normal-sized morphotype of Gephyrocapsa typical of the middle and upper Pleistocene, may substantiate this hypothesis.

The last occurrence of Pseudoemiliania lacunosa (MNN19f/MNN20 zonal boundary) is a synchronous event at a global scale, calibrated to isotopic stage 12 (*Thierstein* et al., 1977) and in the Mediterranean with an age of 0.46–0.47 myr (*Castradori*, 1993). This can be assumed to be the oldest possible age for core 2.

The nannofossil biostratigraphy age of over 0.5 Ma reported for this core by *Bernasconi* et al. (1981) can thus be rejected on the basis of these new results (see also the 1110–1106 m interval).

Interval from 1110 to 1106 m. Two samples (cuttings at 1106 and 1110 m) were analyzed from this interval. Calcareous nannofossil assemblages are poor and rather badly preserved. Based on the absence of Pseudoemiliania lacunosa, coupled with the presence of rare normal-sized Gephyrocapsa, the interval has tentatively been assigned to Zones MNN20–MNN21 of the Middle-Upper Pleistocene (*Rio* et al., 1990).

Interval from 1370 to 1458 m. Four samples from this interval were analyzed (cuttings at 1370, 1400, 1430 and 1458 m). The samples from 1370, 1400 and 1458 m are virtually barren. The 1430 m sample is characterized by a poor, but distinctive nannofossil assemblage. Numerous specimens of Pseudoemiliania lacunosa suggest a stratigraphic position preceding the last occurrence of this species (isotopic stage 12). The absence of normal-sized Gephyrocapsa and the presence of some specimens of small Gephyrocapsa may tentatively narrow its stratigraphic position to the MNN19e Zone (small Gephyrocapsa Zone). Accordingly, the interval could be assigned an age of 0.98–1.24 myr (*Sprovieri*, 1993; *Castradori*, 1993; *Raffi* et al., 1993).

An age of 0.9–1.1 myr was suggested by *Bernasconi* et al. (1981) on the basis of nannoplankton analyses. This age most probably corresponds to the biochronological estimate of the small Gephyrocapsa Zone, as reported by most time-scales in the early eighties, and can thus be considered equivalent to the new results presented here.

Correlation with outcrops

Within the uppermost 400 m of the Trecase 1 sequence, the most interesting volcanic horizons are clearly those between 290 and 345 m and between 250 and 290 m.

From a general point of view, it is difficult to assign a cutting interval to a precise outcropping stratigraphic unit with certainty, because many macroscopic characteristics can not be observed. The prospects for arriving at correlations in such cases are thus necessarily based on the physical, mineralogical and chemical characteristics of the single clasts.

As a first approach, the tephra deposit from between 290 and 345 m has a stratigraphic position and thickness that seem compatible with the CI eruption pyroclastic flow (*Rosi* et al., 1996) and related fallout deposit (*Rosi* et al., 1999). Despite the rejection by *Fisher* et al. (1993), of CI deposition in the Gulf of Naples, the presence of this important (up to 160 m thick) pyroclastic deposit in this area has also been evidenced on the basis of Sparker profiles (*Fusi* et al., 1991; *Milia*, 1998; *Milia* et al., 1998). In *Bernasconi* et al. (1981) and *Balducci* et al. (1983) the presence of CI in the Trecase 1 well was not clearly recognized. On the basis of these authors' lithological and mineralogical description, *Principe* et al. (1987) hypothesized the presence of CI in the depth range of either 325 to 400 m or 325 to 510 m.

The second important volcanic horizon, the fallout layer at 275–290 m, contains both white subaphyric pumices, porphyritic sanidine and fragments of brown glass, characteristics that lead to a first tentative correlation with the Eu-2 member of the Pomici di Base Vesuvian eruption (hereafter PB), as defined by *Bertagnini* et al. (1998).

In order to check both these correlations, microprobe analyses were carried out on the pumice glass of the tuffs from 290 and 340 m, the fallout layer between 275 and 290 m, and the white pumice glass of the Eu-2b member of the PB (Vesuvius), as well as on the Pomici Principali Phlegraean eruption. The results of these new analyses (Tables 6a, b, c) have been compared (Figs. 4 and 5) with the chemical compositions of pumice glasses of the major Vesuvius and Phlegraean Field

Table 6. **a–c** *Microprobe glass analyses. (n) = number of analyses; average values and mean standard deviations are shown for each oxide*. **a** *pumice glasses of 305, 310 and 315 m depth cuttings*. **b** *analyses of white pumices and brown glass fragments from the 275 m depth cutting* **c** *analyses of white pumice from the Pomici Principali, Pomici di Base and Codola eruptions. Analyses were performed on a JEOL JX 8600 electron microprobe at the CSMGA-CNR in Florence. Acceleration voltage was 15 kV, beam current 10 nA, beam diameter 10* µm. *Vitrophyre CFA47 from surges of the Vita Fumo tuff cone (Phlegraean Fields) was used for calibration (Metrich and Clocchiatti, 1989)*

Table 6a

	305–315 m					
	305 m, white pumice $n = 7$		310 m, white pumice $n = 24$		315 m, white pumice $n = 16$	
	Mean	St. Dev.	Mean	St. Dev.	Mean	St. Dev.
SiO_2	60.50	1.01	61.38	1.37	61.34	1.57
TiO_2	0.20	0.28	0.15	0.12	0.14	0.20
Al_2O_3	19.48	3.81	21.98	0.67	20.70	0.63
FeO	0.29	0.03	0.64	0.89	1.02	1.32
MnO	0.07	0.09	0.02	0.05	0.03	0.07
MgO	3.83	0.20	0.38	0.17	0.53	0.16
CaO	3.83	3.74	1.67	0.75	2.18	0.69
Na_2O	5.27	0.07	4.53	0.93	4.56	0.30
K_2O	9.74	0.79	9.21	0.89	9.47	0.67
Water by difference	9.02	1.07	7.36	2.05	8.47	1.94

Table 6b

	275 m			
	white pumice $n = 21$		brown glass $n = 9$	
	Mean	St. Dev.	Mean	St. Dev.
SiO_2	58.45	0.24	52.71	0.26
TiO_2	0.48	0.04	0.74	0.05
Al_2O_3	19.31	0.14	18.6	0.23
FeO	3.30	0.17	7.18	0.17
MnO	0.14	0.02	0.19	0.02
MgO	0.41	0.06	1.64	0.1
CaO	3.63	0.13	6.71	0.44
Na_2O	3.99	0.17	3.1	0.12
K_2O	9.22	0.13	7.48	0.38
SrO	0.11	0.06	0.11	0.08
BaO	0.08	0.06	0.22	0.02
F	0.21	0.17	0.19	0.15
SO_3	0.10	0.03	0.07	0.03
P_2O_5	0.00	0.00	0.41	0.05
Cl	0.58	0.03	0.64	0.03
Water by difference	3.22	1.16	1.2	0.48

Table 6c

Pomici Principali eruption	$n=13$		Pomici di Base eruption	$n=4$		Codola eruption	$n=10$	
	Mean	St. Dev.		Mean	St. Dev.		Mean	St. Dev.
SiO_2	61.41	0.3	SiO_2	61.81	0.08	SiO_2	57.28	0.71
TiO_2	0.32	0.02	TiO_2	0.3	0.06	TiO_2	0.54	0.04
Al_2O_3	18.24	0.15	Al_2O_3	18.43	0.07	Al_2O_3	19.81	0.12
FeO	2.7	0.29	FeO	2.74	0.11	FeO	4.10	0.63
MnO	0.17	0.03	MnO	0.16	0.01	MnO	0.14	0.04
MgO	0.26	0.04	MgO	0.26	0.02	MgO	0.73	0.31
CaO	2.62	0.13	CaO	2.66	0.07	CaO	4.72	0.73
Na_2O	4.9	0.37	Na_2O	4.77	0.39	Na_2O	3.58	0.51
K_2O	8.43	0.5	K_2O	7.98	0.44	K_2O	8.37	1.05
F	0.24	0.11	F	0.23	0.11	F	0.00	0.00
Cl	0.72	0.13	Cl	0.72	0.13	Cl	0.39	0.23
Water by difference	2.77	1.41	Water by difference	1.24	1.5	Water by difference	2.99	0.66

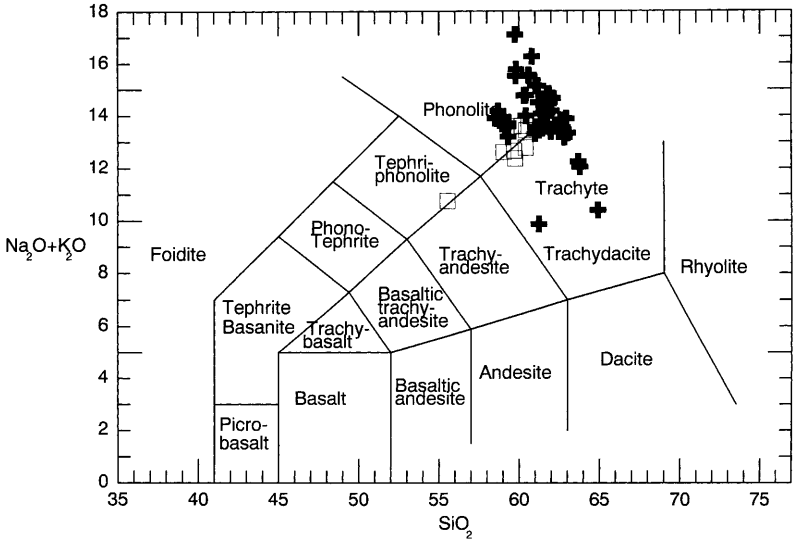

Fig. 4. Total alkali versus silica IUGS classification diagram (*Le Bas* et al., 1986). Average values from glass analyses are indicated. *Crosses*: white pumices from 305, 310 and 315 m depth cuttings; *squares*: Campanian Ignimbrite pumice glasses (*Rosi* and *Sbrana*, 1987; *Vezzoli*, 1991)

eruptions reported in the literature (*Rosi* and *Sbrana*, 1987; *Vezzoli*, 1991; *Rolandi* et al., 1993a, b; *Mues-Schumacher*, 1994; *Cioni* et al., 1995; *Bertagnini* et al., 1998; *Landi* et al., 1999; *Signorelli* et al., 1999a, b).

Pumice compositions in the 290–340 m interval varies from trachitic to phonolitic (Fig. 4). The standard deviations of the average analytical values (Table 6a) reflect the chemical variability of such glasses. The chemical and mineralogical data and the characteristics of the analyzed pumices suggest correlation (Fig. 4) with the data on CI glass (*Rosi* and *Sbrana*, 1987; *Vezzoli*, 1991). The plinian fallout

bed of the same eruption (*Rosi* et al., 1999), which directly underlies the CI further supports this conclusion. No analyses have been performed on this deposit because of the state of alteration of the pumice glass. Microprobe analysis on the fallout pumice glasses (*Signorelli* et al., 1999a) show a variability pattern similar to that of the CI pumices which we analyzed. Finally, the chemical characteristics and the distribution of deposits (*Rosi* and *Sbrana*, 1987; *Milia*, 1998; *Milia* et al., 1998) do not support the presence in the Trecase 1 well of the Neapolitan Yellow Tuff, the only other known deposits with physical characteristics similar to those of the 290–340 m depth tuff.

The white pumice glass at 275–290 m has a phonolitic composition (Fig. 5). The fragments of brown glass also present in this level are instead tephri-phonolitic in composition (Fig. 5). Chemical data related to the Pomici di Base (PB) deposits (*Bertagnini* et al., 1998; *Landi* et al., 1999) indicate a wide range of variability for the products of that eruption. Microprobe data related to the dark glasses of the PB latitic phase are not available in the literature. Both datasets presented in this paper, that on the Trecase 1 well samples, as well as that on the glasses of PB pumice member Eu-2b, demonstrate remarkable differences, especially in terms of alkali and alumina contents (Table 6b and c). On the other hand, the results of the analyses performed on the glasses of the Eu-2b member are in good agreement with other microprobe data in the literature (*Landi* et al., 1999). It can therefore be concluded that the tuff and fallout layer from 275 and 290 m depth can not be correlated with the Somma-Vesuvius PB eruption.

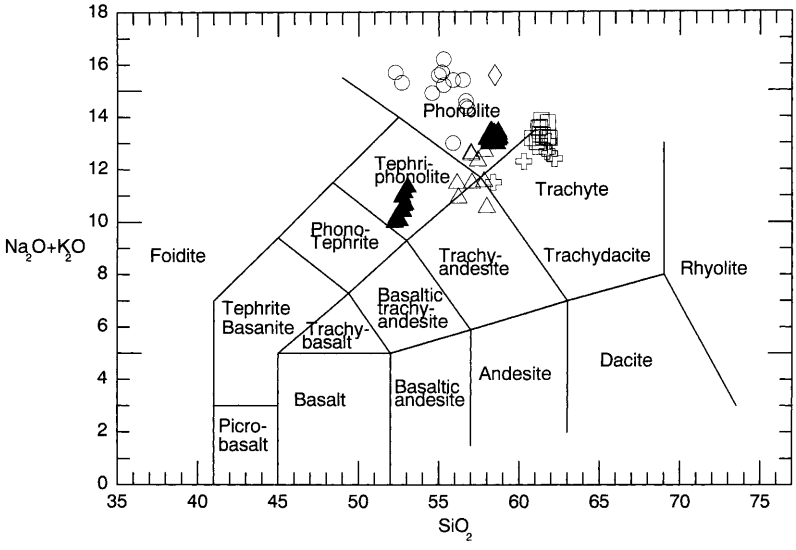

Fig. 5. Total alkali versus silica IUGS classification diagram (*Le Bas* et al., 1986). Average values from glass analyses are indicated. *Filled triangles*: white pumices and brown glass fragments from the 275 m cutting (present work); *open triangles*: Codola pumices (present work); *crosses*: Pomici di Base white pumices (data from present work, *Bertagnini* et al., 1998, *Landi* et al., 1999); *open circles*: 79 AD. white and gray pumices (*Cioni* et al., 1995; *Mues-Schumacher*, 1994) and Avellino white and gray pumices (*Signorelli* et al., 1999); *squares*: Pomici Principali pumices (present work); *diamond*: Mercato pumices (*Rolandi* et al., 1993a)

Comparative microprobe analyses performed on the Pomici Principali glasses (Phlegraean Fields) indicate that there is no correlation between this eruption and the 275–290 m fallout deposit of the Trecase 1 well (Fig. 5). Figure 5 also presents the results of microprobe analyses of Mercato pumices (*Rolandi* et al., 1993a) and Pompeii white and gray pumices (*Mues-Shumacher*, 1994; *Cioni* et al., 1995). The compositions are quite distinct from those of the Trecase 1 fallout. Finally, correlations with the Avellino pumices (*Rolandi* et al., 1993b; *Signorelli* et al., 1999b) have been excluded on the grounds of chemical (Fig. 5), morphological and depositional differences. In addition, well-preserved outcrops are found not far from the Trecase 1 well, along a railway cutting in the urban area of Boscotrecase at 60 m a.s.l. Its thickness of only 10 cm is incompatible with the depth and thickness of the Trecase 1 pumice deposit.

The Codola eruption is the only eruption that has characteristics similar to the 275–290 m fallout level of the Trecase 1 well. This eruption was first mentioned and dated (25 100±400 yr B.P.) by *Alessio* et al. (1974), who attributed it to Somma-Vesuvius activity. *Arno* et al. (1987) briefly described its products. The analogies between the products of the Codola eruption and the 275–290 m fallout level include:

- Its stratigraphic position above the CI Phlegraean eruption and below the PB Vesuvian eruption;
- the close association of light-gray pumice and black scoriae; the porphyritic sanidine in its magmatic fraction;
- the lack of leucite-bearing lavas among the lithics;
- glass chemistry ranging from tephri-phonolite to phonolite (Table 6c, Fig. 5).

The current lack of data on the stratigraphic sequence, distribution and physical and chemical characteristics of the deposits of the Codola eruption prohibit better definition of the correlation between this eruption and the 275–290 Trecase 1 deposits.

The huge volume and dispersal pattern of the PB plinian fallout deposit suggest that it should be present in the area of the Trecase 1 well (*Bertagnini* et al., 1998; *Di Vito* et al., 1998b) within the first 200 m, the interval from which no cuttings were recovered. As the argillified cineritic tuff present from 106 to 116 m depth (*Agip*, 1981) can (owing to the presence of leucite phenocrysts) also be attributed to Vesuvius activity predating the PB eruption, the PB deposits should occur between 116 m (104 m a.s.l.) and 200 m (20 m a.s.l.), a range which is consistent with the altitude of outcrops of this eruption in the Campanian Plain (*Bertagnini* et al., 1998; *Di Vito* et al., 1998).

Therefore, the tephritic lavas found between 200 and 250 m depth should also be stratigraphically located between the CI and PB products. The total thickness of the tephritic lava present in the Trecase 1 well is therefore no greater than 100 m. The thickness and stratigraphic position of these lavas suggest a possible correlation with the series of lava flows and small scoria cones related to the deep fracture trend identified by *Di Vito* et al. (1998a).

Conclusions

The carbonate basement at the base of the stratigraphic sequence in the Trecase 1 well consists of micro- and macro-crystalline azoic dolostones of a lagoon

environment (*Bernasconi* et al., 1981). No stratigraphic correlation has been made with the various carbonate formations in the surrounding Apennines because of lack of fossils.

The thick continental conglomerate found in the Trecase 1 well above the basal dolostones may be related to the erosional phases that followed the NW-SE normal faulting of the Tyrrhenian margin of the Apennines during the Early Pleistocene. This caused vertical displacement of thousands of metres and flooding of the Campanian Plain graben. Marine deposits above the conglomerate layers (up to 1490 m), for which nannofossil biostratigraphy yields an age of 0.98–1.24 myr provide evidence for this event.

From the Sicilian to the Middle Pleistocene, a strike-slip tectonic regime was active in this segment of the Apennines. Uplift of the inner belt ceased in the Middle Pleistocene, and NE-SW extensional tectonics now prevailed (*Brancaccio* et al., 1991; *Hippolyte* et al., 1994). The first episode of volcanic activity in the Vesuvian area occurred at this time. The related tephritic lava sequence between 1141 and 1345 m was emplaced in a marine environment and identifies a defined eruption center that was active about 0.4 myr B.P. A second period of intense effusive activity occurred about 0.3 myr B.P. (lava sequence from 700 to 890 m), separated from the previous one by a period of significant detrital deposition.

The composition of volcanic-origin fragments in this detrital interval varies from tephritic to latitic; we thus contend that a number of tephritic effusive centers were active on the Campanian Plain between 0.4 and 0.3 myr B.P., including interbeds of latitic tephra, probably of Phlegraean Fields origin.

This seems to be confirmed by recent data on pyroclastic eruptions outcropping in the Campanian Plain ranging in age from > 0.315 myr to 0.018 myr (*Gans* et al., 1999). These new findings could also explain the presence of volcanic component in the 365–532 m sand succession; they probably are reworked products of the eruptions.

Between 0.4–0.3 myr and the CI eruption, there is no evidence of volcanic activity from centers located in the Vesuvian area. The thick succession of sands between 365 and 700 meters testifies to deposition in a marginal marine environment, with a transition to a shore environment and then to subaerial conditions in the upper part of the sequence. During the last glacial period the sea level progressively dropped to a minimum of −120 m at about 20,000 yr B.P. (*Chappell* et al., 1996). The uplift of the Phlegraean Fields and of the surrounding area due to rising magma triggered the CI eruption at 37,000 yr B.P. Deposition of the 60 m thick CI could have contributed to the emerging shoreline.

Data from *Chappell* et al. (1996) indicate that the sea level at 37,000 yr B.P. was about 80 meters lower than at present. The CI fallout deposit, whose base is 120 metres below the current sea level, rests on top of beach deposits. This suggests that the Trecase 1 area has subsided by 40 m over the last 37,000 yr.

In another sector of the Campanian Plain (some 20 km to the E) the average subsidence rate suggested by the depth of Tyrrhenian deposits is 0.23 mm/yr (*Cinque* et al., 1987; *Brancaccio* et al., 1991; *Albore Livadie* et al., 1989). During the Holocene, however, the rate accelerated, reaching a value of 1.8 mm/yr over the last 5,000 yr (*Brancaccio* et al., 1991).

Considering the minimum subsidence rate (0.23 mm/yr), the bottom of the CI should now be at 90 m below sea level. The hypothetical tectonic lowering of the

southern part of the Somma-Vesuvius Volcanic Complex, explains the morphological asymmetry of the Somma edifice (*Bianco* et al., 1998) can thus be estimated at a maximum of 30 m.

Re-emergence of volcanic activity in the Vesuvian area occurred only after the CI eruption. Magma rose along and at the intersection of linear and curved tectonic and volcanotectonic elements, linked to the preexisting Pleistocene tectonic trend and formation of the huge CI caldera. It gave rise to a number of small lava and scoria edifices, justifying the term ''lava ridges'' identified on top of the CI by *Di Vito* et al. (1998a). One of these tephritic centers lies above the CI deposits under the Trecase 1 well area, as shown by the tephritic lava sequence encountered between 200 and 250 m depth.

Acknowledgements

The authors wish to thank Dr. *M. Cafiero* of the Exploration Services of the AGIP Directorate for providing access to AGIP's archives and Trecase 1 well cuttings and cores. *L. Vezzoli*, *P. Landi* and *A. Bertagnini* have kindly contributed their valuable knowledge of the Phlegraean Fields and Somma-Vesuvius deposits. *R. Carampin* and *F. Olmi* have been invaluable during the microprobe analyses in Padova and Florence. We are also grateful to *O. Giuliani* and *G. De Grandis* of the IGGI for maintaining the Ar/Ar and mineral separation laboratories. Our heartfelt gratitude also goes to *P. Scandone* for his discerning review of the paper's first draft, to *M. Di Paola* for his useful suggestions, and to two *Mineralogy and Petrology* reviewers for their constructive criticism.

The work has been partially funded by the National Group of Volcanology (GNV) of the Italian National Research Council (CNR) and is a part of a PhD thesis (D.B.) at the University of Pisa.

References

Agip (1981) Trecase 1. Rapporto finale. Rapporto interno Agip/Peit, 60 pp

Albore Livadie C, Barra D, Beneduce G, Brancaccio L, Cinque A, Ortolani F, Pagliuca S, Russo F (1989) Evoluzione geomorfologica, neotettonica e vulcanica della pianura costiera del fiume Sarno (Campania) in relazione agli insediamenti anteriori all'eruzione del 79 d.C.. Vulcan Paleog Archeol PACT 10: 237–256

Alessio M, Bella F, Improta S, Belluomini G, Calderoni G, Cortesi C, Turi F (1974) University of Rome Carbon-14 dates XII. Radiocarbon 16–3: 358–367

Andronico D, Calderoni G, Cioni R, Sbrana A, Sulpizio R, Santacroce R (1995) Geological map of Somma-Vesuvius volcano. Period Mineral 64(1–2): 77–78

Balducci S, Vaselli M, Verdiani G (1983) Exploration well in Ottaviano permit, Italy, Trecase 1. European Geothermal Update 3rd Intern Sem Munich, 29 Nov-1 Dec, pp 407–418

Barbieri M, Di Girolamo P, Locardi E, Lombardi G, Stanzione D (1979) Petrology of the calc-alkaline volcanics of the Parete 2 well (Campania, Italy). Period Mineral 48: 53–74

Barra D, Bonaduce G, Brancaccio L, Cinque A, Ortolani F, Pagliuca S, Russo F (1989) Evoluzione geologica olocenica della piana costiera del fiume Sarno (Campania). Mem Soc Geol Ital 42: 255–267

Bellucci F (1994) Nuove conoscenze stratigrafiche sui depositi vulcanici del sottosuolo del settore meridionale della Piana Campana. Boll Soc Geol Ital 113: 395–420

Bellucci F (1998) Nuove conoscenze stratigrafiche sui depositi effusivi ed esplosivi nel sottosuolo dell'area del Somma-Vesuvio. Boll Soc Geol Ital 117: 385–405

Berggren WA, Hilgen FJ, Langereis CG, Kent DV, Obradovich JD, Raffi I, Raymo ME, Shackleton NJ (1995b) Late neogene (pliocene-pleistocene) chronology: new perspectives in high resolution stratigraphy. Geol Soc Am Bull 107: 1272–1287

Bernasconi A, Bruni P, Gorla L, Principe C, Sbrana A (1981) Risultati preliminari dell'esplorazione geotermica profonda nell'area vulcanica del Somma-Vesuvio. Rend Soc Geol Ital 4: 237–240

Berrino G, Corrado G, Riccardi U (1998) Sea gravity data in the Gulf of Naples: a contribution to delineating the structural pattern of the Vesuvian area. J Volcanol Geotherm Res 82: 139–150

Bertagnini A, Landi P, Rosi M, Vigliargio A (1998) The Pomici di Base plinian eruption of Somma-Vesuvius. J Volcanol Geotherm Res 83: 219–239

Bianco F, Castellano M, Milano G, Ventura G, Vilardo G (1998) Somma-Vesuvius stress field induced by regional tectonics: evidences from seismological and mesostructural data. J Volcanol Geotherm Res 82: 199–218

Brancaccio L, Cinque A, Romano P, Rosskopf C, Russo F, Santangelo N, Santo A (1991) Geomorphology and neotectonic evolution of a sector of the Tyrrhenian flank of the Southern Apennines (Region of Naples, Italy). Z Geomorph N F 82: 47–58

Bruno PPG, Cippitelli G, Rapolla A (1998) Seismic study of the Mesozoic carbonate basement around Mt. Somma-Vesuvius, Italy. J Volcanol Geotherm Res 84: 311–322

Cassano E, La Torre P (1987) Geophisics. In: Somma-Vesuvius. Quaderni de La Ricerca Scientifica. CNR Roma 114/8: 175–196

Cassignol C, Gillot PY (1982) Range and effectiveness of unspiked potassium-argon dating: experimental groundwork and applications. In: *Odin GS* (ed) Numerical dating in stratigraphy. Wiley, Chichester, pp 159–179

Castradori D (1993) Calcareous nannofossil biostratigraphy and biochronology in eastern Mediterranean deep-sea cores. Riv Ital Paleont Stratigr 99(1): 107–126

Cebula GT, Kunk MJ, Mehnert HH, Naeser CW, Obradovich JD, Sutter JF (1986) The Fish Canyon Tuff, a potential standard for the $^{40}Ar/^{39}Ar$ and fission track dating methods (Abstract, ICOG IV, 1986). Terra Cognita 6–2: 139–140

Chappel J, Omura A, Esat T, McCulloch M, Pandolfi J, Ota Y, Pillans B (1996) Reconciliation of late Quaternary sea levels derived from coral terraces at Huon Peninsula with deep sea oxygen isotope records. Earth Planet Sci Lett 141: 227–236

Cinque A (1991) La trasgressione Versiliana nella piana del Sarno (Campania). Geogr Fis Dinam Quater 14: 63–71

Cinque A, Alinaghi HH, Laureti L, Russo F (1987) Osservazioni preliminari sull'evoluzione geomorfologica della piana del Sarno (Campania, Appennino Meridionale). Geogr Fis Dinam Quater 10: 161–174

Cinque A, Patacca E, Scandone P, Tozzi M (1993) Quaternary kinematic evolution of the Southern Appenines. Relationships between surface geological features and deep lithospheric structures. Ann Geofis 36(2): 249–259

Cioni R, Civetta L, Marianelli P, Metrich N, Santacroce R, Sbrana A (1995) Compositional layering and syn-eruptive mixing of a periodically refilled shallow magma chamber: the AD 79 plinian eruption of Vesuvius. J Petrol 36–3: 739–776

Deino AL, Courtis GH, Rosi M (1992) $^{40}Ar/^{39}Ar$ dating of Campaniana Ignimbrite, Campanian Region, Italy. International Geological Congress, Kyoto, Japan, 24 Aug–3 Sept, 3, 633

Deino AL, Courtis GH, Southon J, Terrasi F, Campajola L, Orsi G (1994) ^{14}C and $^{40}Ar/^{39}Ar$ dating of the Campanian Ignimbrite, Phlegraean Fields Italy. ICOG, Berkeley, p 77

Delibrias G, Di Paola GM, Rosi M, Santacroce R (1979) La storia eruttiva del complesso vulcanico del Somma Vesuvio ricostruita dalle successioni piroclastiche del Monte Somma. Rend Soc Ital Mineral Petrogr 35–1: 411–438

Di Girolamo P, Nardi G, Rolandi G, Stanzione D (1976) Occurrence of calk-alkaline two-pyroxene andesites from deep bore-holes in the Phlegraean Fields. 1. Petrographic and petrochemical data. Rend Accad Sci Fis Matemat XLIII: 1–29

Di Vito M, Bella G, Sulpizio R, Zanchetta G (1998a) Stratigrafia dei depositi quaternari nel settore sud-orientale della Piana Campana. National Group for Volcanology – Italy (GNV), XIV Conference, Abstracts volume, pp 96–97

Di Vito M, Sulpizio R, Zanchetta G, Calderoni G (1998b) The geology of the South Western Slopes of Somma-Vesuvius, Italy as inferred by borehole stratigraphies and cores. Acta Vulcanol 10(2): 383–393

Finetti I, Morelli C (1974) Esplorazione sismica a riflessione dei Golfi di Napoli e Pozzuoli. Boll Geofis Teorica Appl 16: 175–222

Fisher RV, Orsi G, Ort M, Heiken G (1993) Mobility of a large-volume pyroclastic flow emplacement of the Campanian Ignimbrite, Italy. J Volcanol Geotherm Res 56: 205–220

Fusi N, Mirabile L, Camerlenghi A, Ranieri G (1991) Marine geophysical survey of the Gulf of Naples (Italy): relationship between submarine volcanic activity and sedimentation. Mem Soc Geol Ital 47: 95–114

Gans PB, Calvert A, Belkin H, Bohrson W, De Vivo B, Rolandi G, Spera F (1999) Eruptive history of the Campanian Ignimbrite(s), Italy, from $^{40}Ar/^{39}Ar$ dating. Geol Soc Am, Cordilleran Section Meeting, Abstracts, Vol 31, Number 6, p A-56

Gillot PY, Chiesa S, Pasquare G, Vezzoli L (1982) <33,000 yr K/Ar dating of the volcanotectonic horst of the Isle of Ischia, Gulf of Naples. Nature 299: 242–245

Hall CH, Farrell JW (1995) Laser $^{40}Ar/^{39}Ar$ ages of tephra from Indian Ocean deep-sea sediments: tie points for the Astronomical and Geomagnetic Polarity Time Scale. Earth Planet Sci Lett 133: 327–338

Hilgen FJ (1991a) Astronomical calibration of Gauss to Matuyama sapropels in the Mediterranean and implication for the Geomagnetic Polarity Time Scale. Earth Planet Sci Lett 104: 226–244

Hilgen FJ (1991b) Extension of the astronomically calibrated (polarity) time scale to the Miocene/Pliocene boundary. Earth Planet Sci Lett 107: 349–368

Hyppolite JC, Angelier J, Roure F (1994) A major geodynamic change revealed by Quaternary stress patterns in the Southern Apennines. Tectonophysics 230: 199–210

Imbrie J, Hays JD, Martinson DG, McIntyre A, Mix AC, Morley JJ, Pisias NG, Prell WL, Shackleton NJ (1984) The orbital theory of Pleistocene climate: support from a revised chronology of the marine 180 record. In: *Berger AL* et al. (eds) Milankovitch and Climate, part I, pp 269–305

Ippolito F, Ortolani F, Russo M (1973) Struttura marginale tirrenica dell'Appennino Campano: reinterpretazione di dati di antiche ricerche di idrocarburi. Mem Soc Geol Ital 12: 227–250

Lanphere MA, Sawyer DA, Fleck RJ (1990) High resolution $^{40}Ar/^{39}Ar$ geochronology of Tertiary volcanic rocks, Western USA. ICOG VII Geol Soc Austr: 27–57

Landi P, Bertagnini A, Rosi M (1999) Chemical zoning and cristallization mechanisms in the magma chamber of the ''Pomici di Base'' plinian eruption of the Somma-Vesuvius (Italy). Contrib Mineral Petrol 135: 179–197

Lourens LJ, Antonarakou A, Hilgen FJ, Van Hoof AAM, Vergnaud-Grazzini C, Zachariasse WJ (1996) Evaluation of the Plio-Pleistocene astronomical timescale. Paleoceanography 11(4): 391–413

Le Bas MJ, Le Maitre RW, Steckeisen A, Zanettin B (1986) A chemical classification of volcanic rocks based on the Total Alkali-Silica diagram. J Petrol 27: 745–750

Metrich N, Clocchiatti R (1989) Melt inclusion investigation of the volatile behaviour in historic alkali basaltic magmas of Etna. Bull Volcanol 51: 185–198

Milia A (1998) Le unit piroclastiche tardo-quaternarie nel Golfo di Napoli. Geogr Fis Dinam Quatern 21: 147–153

Milia A, Mirabile L, Torrente MM, Dvorak JJ (1998) Volcanism offshore of Vesuvius volcano in Naples Bay. Bull Volcanol 59: 404–413

Mues-Schumacher U (1994) Chemical variations of the 79 AD pumice deposits of Vesuvius. Eur J Mineral 6: 387–395

Orsi G, Rosi M (eds) (1991) Large ignimbrite eruptions of the Phlegraean Fields Caldera: the Neapolitan Yellow Tuff and the Campanian Ignimbrite. Workshop on explosive volcanism, Napoli, September 1–8, 1991, Handbook, pp 213

Ortolani F, Aprile F (1978) Nuovi dati sulla struttura profonda della Piana Campana a sud-est del fiume Volturno. Boll Soc Geol Ital 97: 591–608

Principe C, Rosi M, Santacroce R, Sbrana A (1987) Explanatory notes to the geological map. In: *Santacroce R* (ed) Somma-Vesuvius. Quaderni de La Ricerca Scientifica, CNR Roma 114/8: 11–51

Raffi I, Backman J, Rio D, Shackleton NJ (1993) Plio-Pleistocene nannofossil biostratigraphy and calibration to oxygen isotope stratigraphies from DSDP Site 607 and ODP Site 677. Paleoceanography 8(3): 387–408

Rio D, Raffi I, Villa G (1990) Pliocene-Pleistocene calcareous nannofossils distribution patterns in the Western Mediterranean. In: *Kastens KA, Mascle J* et al. (1990) Proc. ODP, Sci Results, 107 (College Station, TX, Ocean Drilling Program): 513–533

Rolandi G, Maraffi S, Petrosino P, Lirer L (1993a) The Ottaviano eruption of Somma-Vesuvio (8000 yr B.P.): a magmatic alternating fall and flow-forming eruption. J Volcanol Geotherm Res 58: 43–65

Rolandi G, Mastrolorenzo G, Barrella AM, Borrelli A (1993b) The Avellino plinian eruption of Somma-Vesuvius (3760 y. B.P.): the progressive evolution from magmatic to hydromagmatic style. J Volcanol Geother Res 58: 67–89

Romano P (1992) La distribuzione dei depositi marini lungo le coste della Campania. Stato delle conoscenze e prospettive di ricerca. Studi Geologici Camerti (spec vol) 1992/1: 265–269

Rosi M, Sbrana A (1987) Phlegraean Fields. Quaderni de ''La Ricerca Scientifica'', CNR Roma 114/9: 175 pp

Rosi M, Sbrana A, Principe C (1983) The Phlegraean Fields: structural evolution, volcanic history and eruptive mechanisms. J Volcanol Geotherm Res 17: 273–288

Rosi M, Vezzoli L, Aleotti P, De Censi M (1996) Interaction between caldera collapse and eruptive dynamics during the Campanian Ignimbrite eruption, Phlegraean Fields, Italy. Bull Volcanol 57: 541–554

Rosi M, Vezzoli L, Castelmenzano A, Grieco G (1999) Plinian pumice fall deposits of the Campanian Ignimbrite eruption (Phlegraean Fields, Italy). J Volcanol Geotherm Res 91: 179–198

Signorelli S, Vaggelli G, Francalanci L, Rosi M (1999a) Origin of magmas feeding the Plinian phase of the campanian Ignimbrite eruption, Phlegraean Fields (Italy): constraints based on matrix-glass and glass-inclusion compositions. J Volcanol Geotherm Res 91: 199–220

Signorelli S, Vaggelli G, Romano C (1999b) Pre-eruptive volatile (H_2O, F, Cl and S) contents of phonolitic magmas feeding the 3550-year old Avellino eruption from Vesuvius, southern Italy. J Volcanol Geotherm Res 93: 237–256

Shackleton NJ, Berger A, Peltier WR (1990) An alternative astronomical calibration of the lower Pleistocene timescale based on ODP Site 677. Trans Roy Soc Edinburgh: Earth Sci 81: 251–261

Sprovieri R (1992) Mediterranean Pliocene biochronology: a high resolution record based on quantitative planktonic foraminifera distribution. Riv Ital Paleontol Stratigr 98(1): 61–100

Sprovieri R (1993) Pliocene-early Pleistocene Astronomically forced planktonic foraminifera abundance fluctuations and chronology of Mediterranean calcareous plankton bioevents. Riv Ital Paleontol Stratigr 99(3): 371–414

Tauxe L, Deino AD, Behrensmeyer AK, Potts R (1992) Pinning down the Bhrunes/Matuyama and upper Jaramillo boundaries: a reconciliation of orbital and isotopic time scales. Earth Planet Sci Lett 109: 561–572

Thierstein HR, Geitzenauer KR, Molfino B, Shackleton NJ (1977) Global synchroneity of Late Quaternary coccolith datum levels: validation by oxygen isotopes. Geology 5: 400–404

Vezzoli L (1991) Tephra layers in Bannock Basin (Eastern Mediterranean). Marine Geol 100: 21–34

Authors' addresses: *D. Brocchini*, Via Petrarca 81, I-57025 Piombino (LI), Italy, e-mail: debora.irene@tiscalinet.it; *C. Principe* (corresponding author) and *M. A. Laurenzi*, Istituto di Geoscienze e Georisorse, Area della Ricerca CNR di Pisa S. Cataldo, via G. Moruzzi 1, I-56124 Pisa (PI), Italy, e-mail: c.principe@iggi.pi.cnr.it; m.laurenzi@iggi.pi.cnr.it; *D. Castradori* and *L. Gorla*, AGIP S.p.A, I-20097 San Donato Milanese, Italy, e-mail: davide.castradori@agip.it; luciano.gorla@agip.it

Appendix 1

$^{40}Ar/^{39}Ar$ Analytical methods

Considering the mineralogy and degree of alteration of the cores, it was decided to carry out whole-rock dating of the lavas sampled at 726 m and 1221 m depths and the lava groundmass from 727 m depth. Samples were irradiated in the F position of the Triga Mark II reactor at the University of Pavia. The vertical flux variation was monitored by the interposition between samples of Fish Canyon Tuff biotite (FCT) as age monitors.

A value of 27.55 myr (*Lanphere* et al., 1990) has been used for the FCT biotite. However, ages have also been recalculated (Table 5) using the value most frequently applied by stratigraphers, i.e. 27.84 myr (*Cebula* et al., 1986). Samples were preheated overnight at a temperature of about 100 °C to eliminate atmospheric Ar on the surface, and subsequently heated in an induction furnace in 25 minutes steps at increasing temperatures until melting. The series of blanks analyzed prior to each sample had an atmospheric composition. The data obtained have been corrected for instrumental background, isotopic fractionation, ^{37}Ar decay and interference of Ar isotopes produced during irradiation by reactions involving K, Ca and Cl.

Ages have been calculated as plateau ages (Fig. 3) by accounting for analytical error alone. Other sources of error (neutron flux variations, uncertainty concerning the age of the monitor) have been taken into account subsequently. The plateau has been determined by the weighted average of the ages of at least three consecutive steps yielding the same age within the analytical limits of 2σ and representing at least 50% of the gas released (assuming the initial composition of the system to be atmospheric). The high atmospheric Ar content of these samples has excluded age calculation by means of the isotopic correlation diagram ^{39}Ar/^{40}Ar vs ^{36}Ar/^{40}Ar (''inverse'' isochron). In fact, the points tend to concentrate very close to the ^{36}Ar/^{40}Ar axis, resulting in an ill-defined isochron.

Table A1. *$^{40}Ar/^{39}Ar$ stepwise heating data. Isotope concentrations are in ml/g. They have been corrected for dynamical background, isotopic fractionation and ^{37}Ar decay only. Mass interference corrections have been computed in the age calculations. The correction factors used are: $(^{36}Ar/^{37}Ar)_{Ca} = 0.00026$, $(^{39}Ar/^{37}Ar)_{Ca} = 0.00067$, $(^{40}Ar/^{39}Ar)_K = 0.02$. The errors shown are $\pm 1\sigma$, while errors in the plateau ages include uncertainty in monitor measures and age as well as vertical neutron flux variations*

TC1, 726m WR		J = 2.818E-04					Weight = 144 mg					
T(°C)	$^{40}Ar_{tot}$	Err	^{39}Ar	Err	^{38}Ar	Err	^{37}Ar	Err	^{36}Ar	Err	Age (myr)	Err
520	8,112E-07	1,989E-09	3,159E-10	5,449E-12	4,953E-10	5,252E-12	2,261E-10	1,632E-11	2,698E-09	1,804E-11	22,2605	8,4848
580	3,396E-06	1,658E-08	3,971E-09	2,452E-11	2,251E-09	2,949E-11	3,652E-09	3,42E-11	1,111E-08	8,507E-11	14,2827	3,1970
650	1,457E-06	3,606E-09	1,171E-08	4,692E-11	1,015E-09	1,188E-11	6,476E-09	4,602E-11	4,638E-09	2,8E-11	3,7612	0,3590
710	1,409E-06	4,548E-09	4,257E-08	1,244E-10	1,385E-09	1,164E-11	1,217E-08	7,539E-11	4,515E-09	3,213E-11	0,8992	0,1133
780	1,515E-06	4,789E-09	7,158E-08	2,381E-10	1,849E-09	1,842E-11	1,81E-08	1,195E-10	4,837E-09	4,025E-11	0,6216	0,0844
840	1,132E-06	3,206E-09	6,317E-08	2,371E-10	1,464E-09	1,281E-11	1,568E-08	1,077E-10	3,616E-09	2,275E-11	0,5209	0,0541
910	8,294E-07	2,735E-09	5,79E-08	1,743E-10	1,196E-09	1,284E-11	1,547E-08	9,312E-11	2,72E-09	1,822E-11	0,2358	0,0472
970	7,970E-07	2,048E-09	6,029E-08	2,019E-10	1,242E-09	1,048E-11	1,852E-08	1,307E-10	2,588E-09	1,812E-11	0,2830	0,0451
1140	2,734E-06	9,485E-09	1,651E-07	4,406E-10	3,769E-09	2,284E-11	1,377E-07	7,979E-10	8,919E-09	7,231E-11	0,3351	0,0656
1300	3,849E-07	7,222E-10	3,075E-08	9,235E-11	6,126E-10	5,147E-12	3,105E-08	1,808E-10	1,231E-09	1,097E-11	0,3894	0,0533
1560	5,612E-07	1,024E-09	8,868E-09	3,639E-11	4,548E-10	5,283E-12	1,002E-08	6,466E-11	1,855E-09	1,675E-11	0,7980	0,2835
Plateau age (910–1300 °C) = 0,305±0,045 myr												

TC1, 727m, GM		J = 2.978E-04					Weight = 104 mg					
T(°C)	$^{40}Ar_{tot}$	Err	^{39}Ar	Err	^{38}Ar	Err	^{37}Ar	Err	^{36}Ar	Err	Age (myr)	Err
520	6,04E-08	2,05E-10	2,76E-10	3,23E-12	4,00E-11	9,71E-13	1,15E-10	2,32E-12	1,89E-10	2,25E-12	8,601	1,291
580	1,72E-07	5,31E-09	1,29E-09	3,46E-11	1,25E-10	4,00E-12	5,48E-10	1,60E-11	5,50E-10	1,60E-11	3,898	1,964
650	1,37E-07	1,87E-10	1,93E-09	9,90E-12	1,08E-10	1,18E-12	1,35E-09	9,71E-12	4,46E-10	4,74E-12	1,447	0,389
780	1,50E-07	3,73E-10	5,67E-09	1,95E-11	1,63E-10	1,50E-12	4,89E-09	2,43E-11	4,90E-10	4,49E-12	0,549	0,125
940	5,88E-07	2,98E-09	4,05E-08	1,43E-10	8,48E-10	5,24E-12	1,45E-08	9,31E-11	1,90E-09	1,46E-11	0,335	0,057
1070	4,17E-07	1,13E-09	3,02E-08	4,96E-10	6,30E-10	1,21E-11	1,71E-08	2,02E-10	1,36E-09	7,13E-12	0,298	0,038
1070	6,15E-08	3,42E-10	2,79E-09	1,73E-11	6,90E-11	9,22E-13	2,24E-09	2,05E-11	2,02E-10	1,65E-12	0,385	0,094
1140	2,82E-08	7,74E-11	1,59E-09	4,94E-12	3,62E-11	1,21E-12	1,78E-09	1,71E-11	9,13E-11	1,33E-12	0,437	0,133
1200	1,70E-08	3,81E-11	7,24E-10	3,74E-12	1,85E-11	9,71E-13	9,90E-10	8,28E-12	5,30E-11	6,77E-13	1,092	0,148
1300	1,61E-08	3,37E-11	4,88E-10	3,89E-12	1,40E-11	7,89E-13	6,04E-10	7,42E-12	5,17E-11	1,18E-12	0,935	0,384
1450	4,70E-08	1,38E-10	1,07E-09	5,27E-12	4,46E-11	1,74E-12	1,17E-09	1,05E-11	1,55E-10	2,49E-12	0,680	0,369
1560	1,11E-07	3,84E-10	1,27E-11	5,74E-13	6,83E-11	1,81E-12	1,99E-11	2,01E-12	3,71E-10	4,05E-12	19,664	50,081
Plateau age (940–1140 °C) = 0,323±0,032 myr												

TC1, 1221, WR		J = 2.858E-04					Weight = 138 mg					
T(°C)	$^{40}Ar_{tot}$	Err	^{39}Ar	Err	^{38}Ar	Err	^{37}Ar	Err	^{36}Ar	Err	Age (myr)	Err
520	1,43E-07	3,166E-10	1,897E-09	7,464E-12	1,112E-10	1,12E-12	1,068E-10	2,42E-12	4,714E-10	3,49E-12	1,1130	0,2802
580	4,39E-07	2,025E-09	1,517E-08	5,304E-11	4,524E-10	3,36E-12	8,547E-10	9,095E-12	1,439E-09	1,166E-11	0,4631	0,1171
650	2,34E-07	6,484E-10	1,514E-08	3,957E-11	3,511E-10	2,52E-12	1,057E-09	7,929E-12	7,591E-10	4,898E-12	0,3358	0,0493
710	1,61E-07	4,022E-10	9,334E-09	2,839E-11	2,845E-10	2,47E-12	1,601E-09	1,189E-11	5,239E-10	4,318E-12	0,3365	0,0704
780	1,58E-07	2,686E-10	5,531E-09	1,993E-11	2,927E-10	2,51E-12	2,097E-09	1,421E-11	5,219E-10	3,564E-12	0,4067	0,0981
840	6,99E-07	2,684E-09	2,994E-08	7,619E-11	1,301E-09	5,844E-12	1,126E-08	7,776E-11	2,296E-09	1,751E-11	0,3691	0,0890
910	1,25E-07	3,17E-10	6,658E-09	1,669E-11	1,956E-10	2,25E-12	3,918E-09	1,995E-11	4,079E-10	3,03E-12	0,3966	0,0692
970	7,84E-08	1,26E-10	3,536E-09	9,375E-12	9,626E-11	6,15E-13	3,783E-09	2,227E-11	2,554E-10	1,75E-12	0,4668	0,0751
1140	1,05E-07	2,524E-10	3,392E-09	1,373E-11	1,208E-10	1,35E-12	2,82E-08	1,804E-10	3,524E-10	2,80E-12	0,4665	0,1240
1300	2,62E-08	4,584E-11	8,912E-10	4,286E-12	3,184E-11	7,13E-13	8,313E-09	6,006E-11	8,639E-11	1,24E-12	0,7503	0,2088
1560	5,12E-08	1,018E-10	1,388E-10	1,42E-12	3,319E-11	5,757E-13	1,267E-09	1,082E-11	1,725E-10	1,62E-12	1,3836	1,7814
Plateau age (580–910 °C) = 0,361±0,026 myr												